ELSEVIER

Marine Geology 177 (2001) 111–128

MARINE GEOLOGY
INTERNATIONAL JOURNAL OF MARINE GEOLOGY, GEOCHEMISTRY AND GEOPHYSICS

www.elsevier.nl/locate/margeo

Early diagenetic processes in the muddy sediments of the Bay of Biscay

C. Hyacinthe[1], P. Anschutz*, P. Carbonel, J.-M. Jouanneau, F.J. Jorissen

Université Bordeaux 1, Departement de Geologie et Oceanographie (D.G.O.), CNRS UMR 5805, 33405 Talence Cedex, France

Received 23 September 1999; accepted 29 December 2000

Abstract

In order to understand the early diagenesis processes occurring in continental margin environment, modern sediments collected in six different sites from the Bay of Biscay have been studied. These sites can be separated into two groups. In the shallowest stations, where sediments are highly bioturbated, organic carbon levels are higher than 2%. In the deepest stations, sediments are much less bioturbated, and organic carbon levels are lower. In all sites, the vertical distribution of redox sensitive species can be explained by the well-established depth sequence of redox reactions, based on the bacterially mediated oxidation of organic matter. We have considered some alternative reaction pathways to explain the profiles of Fe, Mn, and N species. These reactions deal with the ammonia oxidation by manganese oxide, the aerobic denitrification and the oxidation of dissolved iron (II) by nitrate or Mn-oxides. Vertical flux calculations with a simple diffusion model indicate that these reactions could account for the reduction of all the Mn-oxides and the oxidation of all the upward diffusing Fe(II). They may also be responsible for a significant part of the total dinitrogen production. The relative importance of these pathways on early diagenetic processes and benthic fluxes has not been determined and must be examined with additional experimental works. Our study suggests, however, that the coupling between the benthic cycles of iron, manganese and nitrogen could strongly influence the carbon cycling at the ocean floor.

Keywords: Geochemistry; Sediment; Early diagenesis; Bay of Biscay; Manganese; Iron; Nitrogen

1. Introduction

Modern oceanic sediments comprise the first decimetres below the sediment–water interface. This compartment contains organic carbon recently imported from the overlying water column. This carbon sustains biogeochemical reactions, which are important for the oceanic budget of C, N, P, and S species, and for some metals, such as Mn and Fe. Continental margin sediments play an important role, because their organic carbon content is much higher than in deep oceanic sediments. The mineralization of organic carbon alters the initial mineralogy and chemistry of deposited particles and interstitial waters, and determines the benthic cycle of redox species and the fate of sedimentary organic matter. The early diagenetic processes are mostly driven by the biological activity of the

* Corresponding author. Tel.: +33-556-848873; fax: +33-556-840848.

E-mail address: anschutz@geocean.u-bordeaux.fr (P. Anschutz).

[1] Present address: Faculty of Earth Sciences, Department of Geochemistry, Budapestlaan 4, 3584 CD Utrecht, The Netherlands.

0025-3227/01/$ - see front matter
PII: S0025-3227(01)00127-X

micro-organisms present in the modern sediments. The bacterially-mediated oxidation of organic matter is reflected in a well-established depth sequence of redox reactions in which oxygen is reduced near the sediment–water interface, followed by the reduction of nitrate, manganese- and reactive iron-oxides, sulfate, and finally carbon dioxide (Froelich et al., 1979; Postma and Jakobsen, 1996). The production of reduced compounds during the anaerobic degradation of organic matter can also play a major role in the reduction of oxidants (Canfield et al., 1993). Several multicomponent early diagenetic models have been developed that explicitly describe the coupling of the cycles of Mn and Fe to those of O_2, C, S, and N (Burdige and Gieskes, 1983; Boudreau, 1996; Wang and Van Cappellen, 1996). In the web of possible reactions, recent studies attach more and more importance to metal oxides, particularly for their role in the benthic cycle of nitrogen (Luther et al., 1997; Aller et al., 1998; Anschutz et al., 2000). It has been pointed out by different authors that the reduction of Mn-oxide by diffusing ammonia could be an important process of dinitrogen or nitrate production (e.g. Hulth et al., 1999; Anschutz et al., 2000). This pathway could interfere with dissimilatory Mn-reduction. The aim of the present study was to test the possibility of adding strong interactions between iron, manganese and nitrogen in the interpretation of the vertical distribution of redox species in modern sediment. The study is based on measurements in sediments of the Aquitaine margin in the Bay of Biscay of vertical profiles of the major chemical species that enter in early diagenesis. We have studied six sediment cores collected between 150 and 2800 m depth in order to test the importance of the different reactions in several environmental conditions, differing by the content of organic matter, the sedimentation rate, and bioturbation intensity. The semi-quantitative approach is based on vertical flux calculations. It has been carried out in order to estimate the potential role of different redox reactions that are thermodynamically feasible, in which reduced products (Fe^{2+}, Mn^{2+}, and NH_4^+) interact with oxidants (O_2, NO_3^-, Fe- and Mn-oxides). This study is a part of the program Oxybent, which aims at understanding the mechanisms of benthic biogeochemistry and their role in the fossilisation of sedimentary signals.

2. Material and methods

2.1. Sampling location

The studied sediments have been collected in the southeastern part of the Bay of Biscay (Fig.1) on the slope of the Aquitaine margin (stations A, B, and D) and on flat parts of the canyon of Capbreton (stations C and E) and Cap Ferret (Stn. I). The sediments of the stations located above 700 m (D, C, and B) are in contact with North Atlantic Central Waters, whereas stations E and A are under the influence of the vein of Mediterranean waters. The temperature of both water masses ranges between 10.5 and 13°C. The bottom of station I is overlaid by North Atlantic Deep Waters, with a temperature of 4°C. In all the stations, the sediment consists of mud composed of clay, silt, and less than 30% carbonates. The clay fraction is dominated by illite, smectites, chlorites, and kaolinites (Latouche et al., 1991).

2.2. Material

The sediments have been collected with a multicorer during cruise Oxybent-7 in January 1999 with the ship 'Côtes de la Manche'. The multi-corer allows to sample the first decimetres of sediments, the overlying bottom waters, and the undisturbed sediment–water interface, in a 10 cm diameter pexiglas tube. Free waters have been collected immediately after core recovery for dissolved O_2 measurements, using the Winkler titration method (Strickland and Parsons, 1972). Profiles of pore water O_2 have been achieved on board using a cathode-type mini-electrode (Revsbech and Jørgensen, 1986; Helder and Bakker, 1985; Revsbech, 1983). The temperature was maintained by using an insulating device. This operation was completed within 15 min after core recovery for sediments where the oxygen penetration depth was the lowest, and less than 30 min for other cores. Subsequently, the core used for O_2 profiling has been sliced in thin horizontal sections (0.5 cm for the top 2 cm, 1 cm below, and 2 cm at the bottom) within 1.5 h. For every level, a sub-sample was immediately sealed in a pre-weighed vial and frozen under inert atmosphere (N_2) for further analyses of porosity and solid fraction. Another sub-sample was centrifuged under N_2 at 5000 rpm during 20 min in order

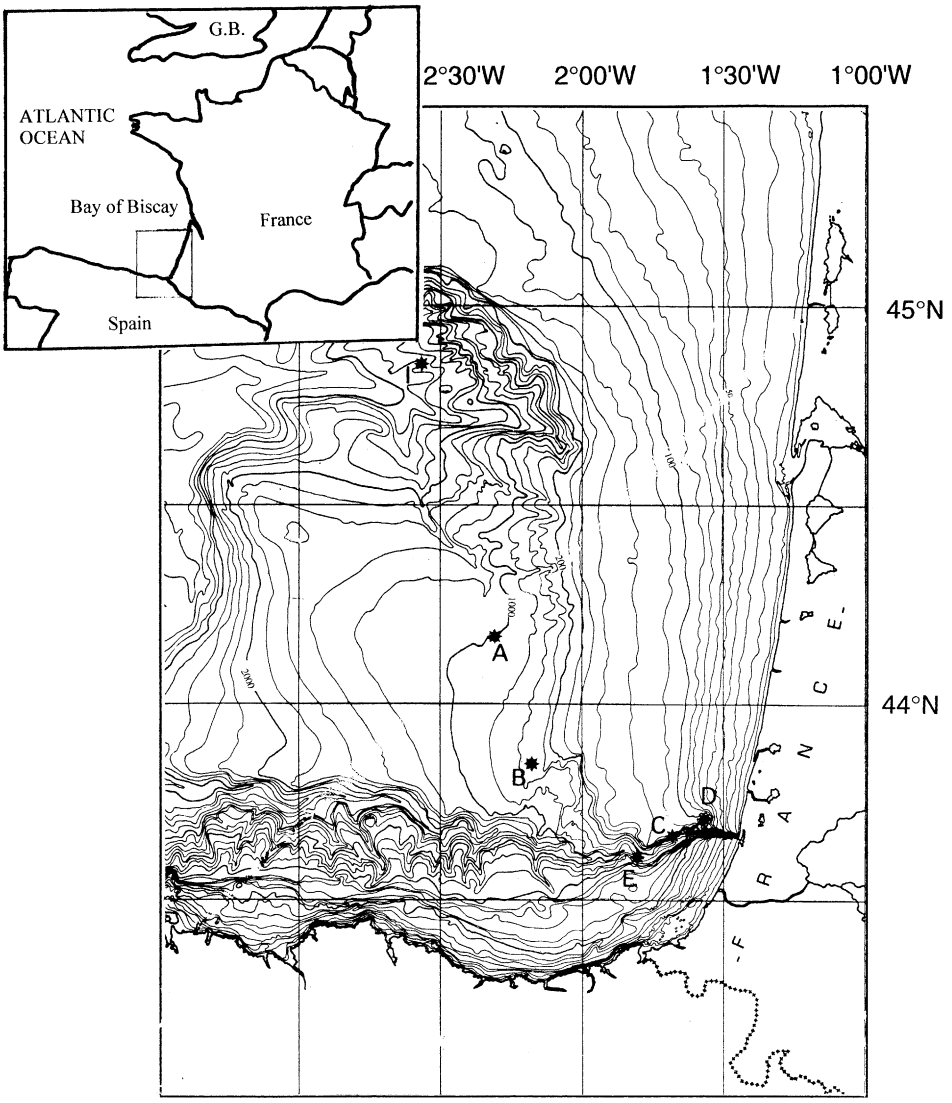

Fig. 1. Map of the Southeastern part of the Bay of Biscay showing the station locations of OXYBENT 7 cruise.

to collect pore waters. Two aliquots of water were filtered (0.2 μm) and frozen at −25°C for nutrient analyses, and another aliquot was filtered and acidified with ultrapur HNO_3 for dissolved Mn and Fe analyses. Surface sediment from a second core was collected for ^{210}Pb analysis. The complete vertical profiles of ^{210}Pb activity for stations A, B, C, and D were obtained in cores collected at the same locations during mission Oxybent-1 (Anschutz et al., 1999). Surface samples from station E collected during mission Oxybent-2 were also analysed. We noted the presence of polychaetes and burrows down to the bottom of the cores in stations C and D.

2.3. Laboratory analyses

The activities of ^{210}Pb were determined in freeze-dried samples by gamma counting. The excess activities were calculated from ^{226}Ra-supported ^{210}Pb deduced from the activities of ^{214}Pb and ^{214}Bi.

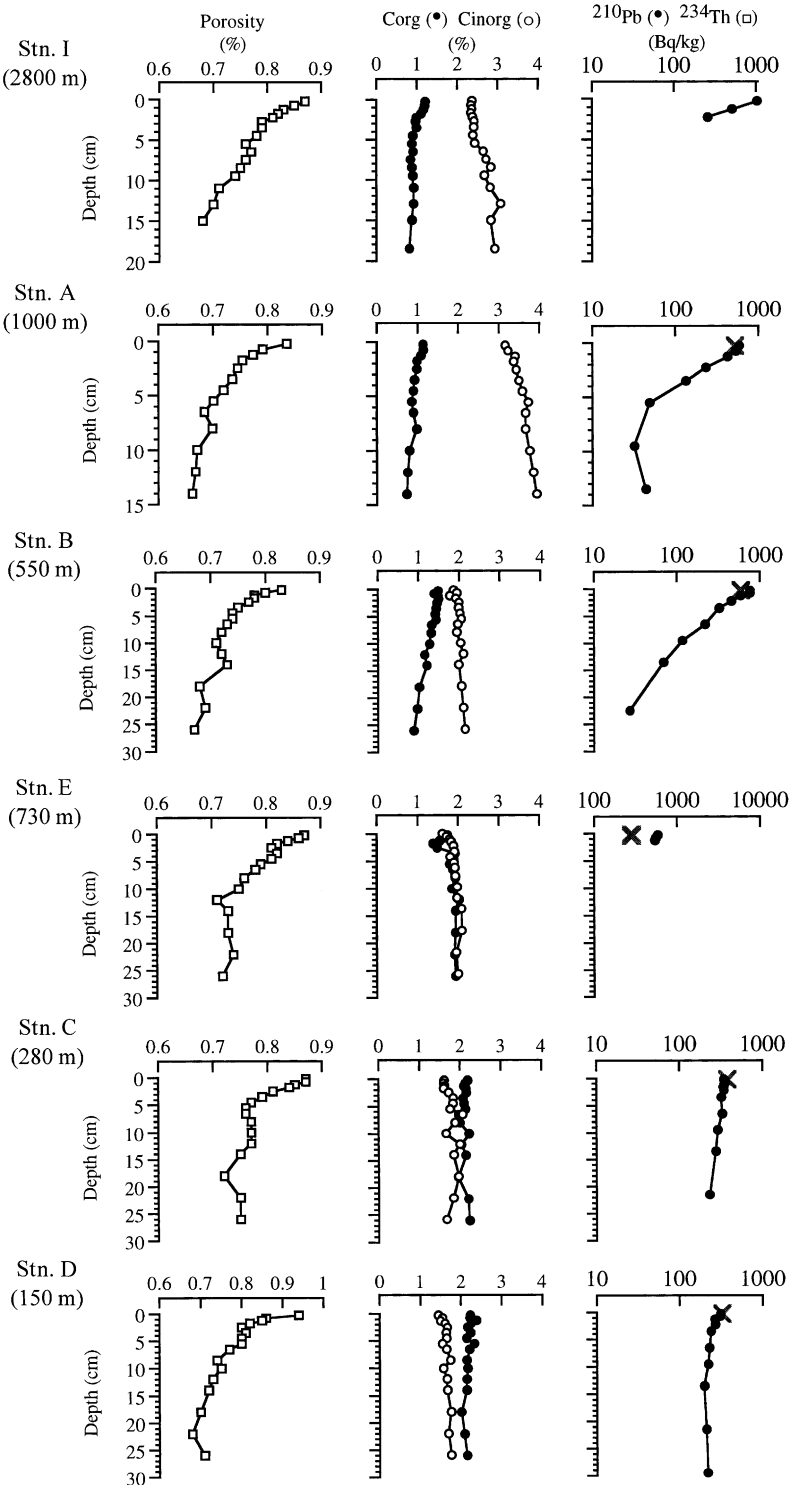
Porosity
(%)
Corg (•) Cinorg (○)
(%)
210Pb (•) 234Th (□)
(Bq/kg)
Stn. I
(2800 m)
Stn. A
(1000 m)
Stn. B
(550 m)
Stn. E
(730 m)
Stn. C
(280 m)
Stn. D
(150 m)
Depth (cm)

Fig. 2.

Porosity was determined by comparison of the weights of wet and freeze-dried sediment. The freeze-dried solid fraction was homogenised and the water content used to correct the analyses for the presence of sea salt.

Particulate sulfur (S_{tot}) and total carbon were measured on the dry sediment using a Leco C/S 125. Organic carbon (C_{org}) was measured after removal of carbonates with 2N HCl from 50 mg of powdered sample. Inorganic carbon (C_{inorg}) is the difference between total carbon and C_{org}. Wet samples were subjected to two different extraction techniques for the determination of reactive particulate Fe and Mn. The most reducible fraction was extracted with an ascorbate solution buffered at pH 8 (Ferdelman, 1988; Kostka and Luther, 1994; Anschutz et al., 1998). A second extraction on a separate aliquot was carried out with 1N HCl to determine acid soluble Mn and Fe. For both procedures, about 1 g of wet sample was leached with a 25 ml solution during 24 h while shaking continuously at room temperature. Iron extracted with ascorbate (Fe_{ASC}) comes from amorphous iron oxides, and it can partly result from the leaching of FeS (Kostka and Luther, 1994). Iron extracted with HCl (Fe_{HCl}) comes from the fraction extracted with ascorbate, FeS, some iron phyllosilicates and carbonates. Specific tests on particulate-Mn extraction with ascorbate (Mn_{ASC}) or 1N HCl (Mn_{HCl}) have not been done yet. It has been shown, however, that Mn_{HCl} was close to total Mn in modern marine sediments (Anschutz et al., 2000). It represents the whole fraction of Mn-oxides and Mn associated with carbonates. Mn_{ASC} is extracted at pH 8, which suggests that Mn-carbonates are not leached. Our results presented here also show that the ascorbate solution extracts less Mn-oxides than HCl. The extracted fraction must correspond to the most reducible particles containing Mn(III,IV). Mn and Fe were measured by flame atomic absorption spectrometry.

Interstitial water compounds were analysed using techniques adapted for small volumes of samples. Nitrate and nitrite were measured by flow injection analysis (FIA) according to Anderson (1979). Ammonia was analysed with the FIA method described by Hall and Aller (1992). Sulfate was measured with a nephelometric method, and Fe^{2+} with the colorimetric method using ferrozine (Stookey, 1970). Dissolved Mn^{2+} was determined by atomic absorption spectrometry.

3. Results

3.1. Activity of ^{210}Pb

The excess activity of ^{210}Pb ($T_{1/2} = 22.3$ years) decreases exponentially below the interface in the deep slope stations (I, A, and B) (Fig. 2), whereas the profiles of ^{210}Pb are almost vertical in stations C and D. The ^{210}Pb activities of surface sediments measured in cores taken during mission Oxybent-7 were close to those measured during previous Oxybent missions, except for station E. Here, activity was lower in January 1999 than 1 year before.

3.2. Pore water composition

The penetration depth of dissolved O_2 ranges between 6 mm in Stn. D and 45 mm in Stn. I (Fig. 3). The profiles of stations I, and B show a sharp gradient of O_2 in the top 5 mm, and a smoother decrease below to total anoxia. The presence of two slopes in the O_2 profiles can be related to many processes, such as to changes with depth of the reactivity of organic matter (Hulthe et al., 1998; Rabouille et al., 1998), porosity changes, or non-steady state.

The concentration of nitrate in the bottom waters of stations I and A is 17 μmol/l (Fig. 4). It is lower for shallower stations. The top sample of the pore water profiles is enriched in NO_3^- relative to the bottom water, which suggests that the sediment was a source of nitrate for the water column in January 1999. NO_3^- drops to concentrations close to zero below the oxic layer. However, nitrate is sporadically present in the anaerobic part of the sediment. When nitrite is detected, the profiles show peaks in the samples containing maximum concentration of nitrate or in

Fig. 2. Vertical profiles of porosity in % (left), organic carbon (Corg) and inorganic carbon (Cinorg) in weight percent of dry sediment corrected for salt content (middle), and excess ^{210}Pb in Bq/kg (right). The ^{210}Pb profiles were obtained from cores collected during the mission Oxybent-1 (October 1997) for stations A, B, C, and D, Oxybent-2 (January 1998) for Stn. E, and Oxybent-7 (January 1999) for Stn. I. The black crosses represent the excess ^{210}Pb data of surface sediments collected during Oxybent-7.

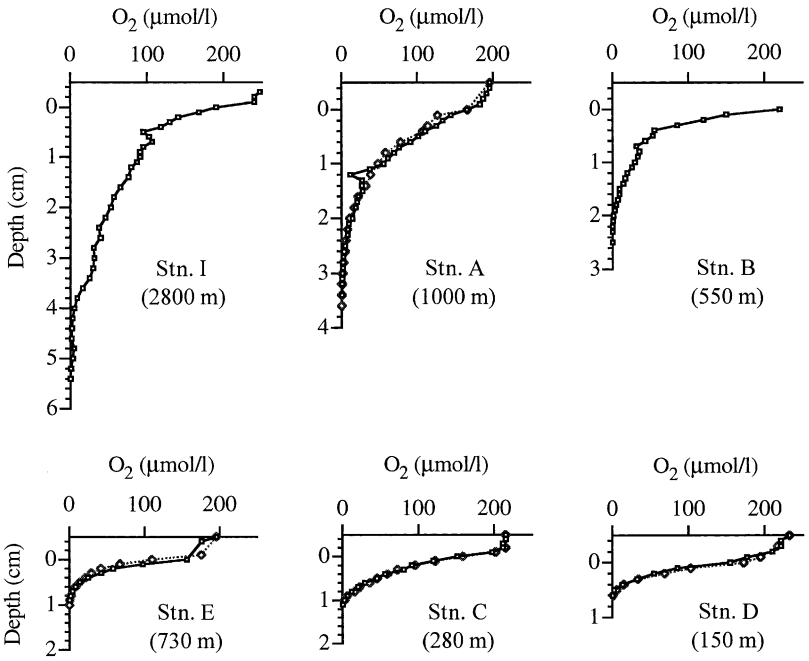

Fig. 3. Vertical profiles of pore water oxygen in μmol/l. For some stations duplicate analyses were performed.

the sample located just below. The NO_3^- profile of Stn. I shows a maximum concentration in the oxic layer at 1 cm. The concentration decreases irregularly below, with two steps between 3 and 5 and 6 and 9 cm. The concentrations of dissolved NH_4^+ are below the detection limit in the bottom water and remain low in the oxic part of the sediment. They increase generally in a regular manner just below. The concentrations are highest at the bottom of the cores, and in the stations enriched in C_{org}.

Dissolved manganese becomes detectable in samples where the oxygen concentration reaches values close to zero. Below, the Mn^{2+} concentrations increase gently with depth in stations I and A, but remain below 30 μmol/l. In stations C, D, and E, the Mn^{2+} profile shows a peak of concentration of about 100–150 μmol/l below the oxic layer, and then, it drops to reach a lower, but constant value. Dissolved iron appears below dissolved manganese, at a level that corresponds to the disappearance of nitrate. The profiles of Fe^{2+} are more scattered than those of Mn^{2+}. Sulfate concentration remains constant and equal to seawater concentration all along the studied cores, except the deepest sample of Stn. D, which shows a slight decrease. Dissolved sulfide has not been analyzed, but the concentrations are probably close to zero, since we noted no smell of sulfide during core processing on board.

The profiles of dissolved species in Stn. B show anomalies between 10 and 15 cm depth (Fig. 4). This interval contained a dead urchin shell and was more fluid than above, as shown in the porosity profile (Fig. 2). The layer contains nitrate and nitrite, whereas the concentrations of Mn^{2+}, Fe^{2+}, and NH_4^+ drop to zero.

3.3. Reactive solid fraction

The concentration of C_{org} for the surface sediment decreases from the shallowest station D (2.23%) to the deepest station I (1.20%) (Fig. 2). C_{org} content decreases slowly downcore in stations I, A, and B. It remains approximately constant in stations C and D. The profile of Stn. E shows a negative anomaly between 1 and 3 cm depth.

The stations I, A, and B contain less than 25 μmol/g of S_{tot} (Fig. 4). The lowest concentrations were measured at the sediment surface. Stations C and D

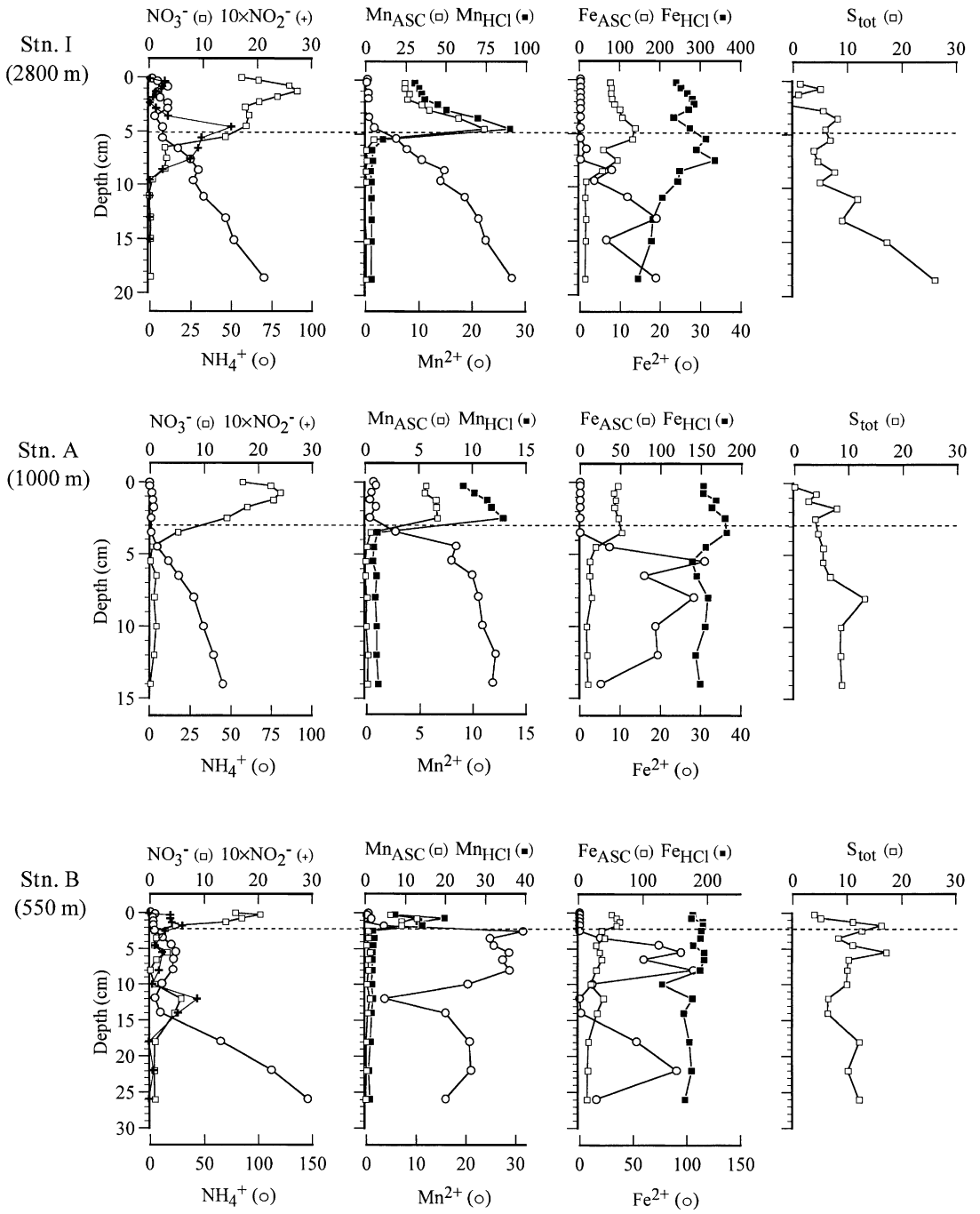

Fig. 4. Vertical profiles of redox sensitive species in modern sediments of the Bay of Biscay. The pore water compounds are given in μmol/l (NO_3^-,NO_2^-, NH_4^+, Mn^{2+}, Fe^{2+}). The value indicated at depth 0 cm represents the value measured in the bottom water. The reactive particulate phases are given in micromole per gram of dry sediment (μmol/g) and correspond to ascorbate and 1N HCl extractable manganese (Mn_{ASC} and Mn_{HCl}) and iron (Fe_{ASC} and Fe_{HCl}), and total sulfur (S_{tot}). The horizontal bar represents the oxygen penetration depth.

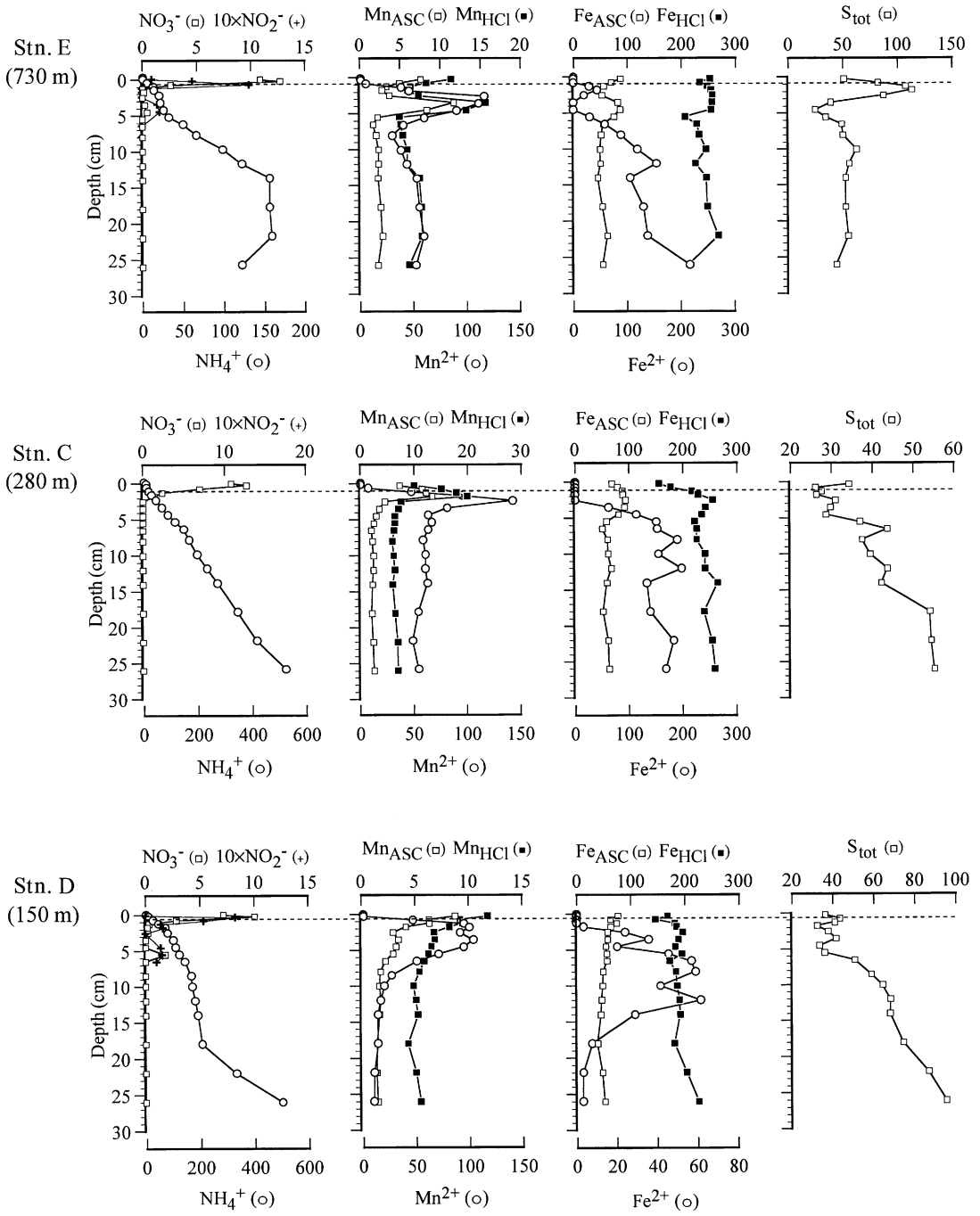

Fig. 4. (*continued*)

contain more than 30 μmol/g of sulfur in the top sample. At depth, the concentration increases up to 95 μmol/g at the bottom of Stn. D. Station E has the highest concentration of sulfur in the subsurface layer poor in C_{org}.

The profiles of Mn_{ASC} and Mn_{HCl} are parallel, with higher concentrations measured for the acid leaching. All profiles show a peak at the surface, with maximum values located at the oxygen penetration depth. In stations I, A, and B, the concentration decreases abruptly below the oxic front, reaching values close to zero. In stations C and D, concentrations decrease more gradually. Mn_{ASC} decreases to values close to zero, whereas Mn_{HCl} remains at concentrations above 5 μmol/g. Fe_{ASC} concentrations in the nitrate containing top layer are close to, or above 50 μmol/g. Extractable iron decreases towards the bottom of the cores in stations I, A, B, and C, whereas the profiles remain relatively linear in Stn. D. The vertical distribution of Fe_{HCl} is similar but the absolute amounts extracted are 100–200 μmol/g higher.

4. Discussion

4.1. Sediment transport and mixing

The decrease in excess activity of ^{210}Pb in the deep slope stations (I, A, and B), suggests that the sediments are little or not mixed by mechanical advection or bioturbation (Fig. 2). The accumulation rates deduced from the slope of the ^{210}Pb profile, the radioactive decay constant, and the porosity, for stations I, A, and B are 24, 51, and 77 mg/cm^2/year, respectively. The profiles of ^{210}Pb are almost vertical in stations C and D, which suggests that they are highly bioturbated down to 30 cm. The presence of polychaetes and burrows down to the bottom of the cores in these stations supports this hypothesis. C_{org} remains constant for stations C and D, which corroborates the hypothesis that the sediment of these stations is well mixed. The ^{210}Pb activity of surface sediments of Stn. E was lower in January 1999 than 1 year before. Station E is located in the talweg of the Capbreton canyon, which can be exposed to episodic gravitational input of downsloping sediment. The top of the Station E core can consist of a ^{210}Pb-depleted and recently deposited sediment layer.

4.2. The redox sequence of degradation of organic matter

We observe that the oxygen concentration decreases rapidly below the sediment surface. Nitrate increases in the oxygen containing layer and then decreases below. The disappearance of oxygen and nitrate is accompanied by a decline of the Mn-oxide content and an increase in dissolved manganese, followed deeper down by an increase in dissolved iron. Total sulfur content increases with depth. This distribution follows the well-established depth sequence of diagenetic reactions governed by the preferential use of the electron acceptor that yields the highest amount of free energy for the bacterially mediated oxidation of organic matter. Oxygen is reduced near the sediment–water interface, followed by the reduction of nitrate and manganese oxide, then reactive iron oxide (Fe_{ASC}), and sulfate (Froelich et al., 1979; Postma and Jakobsen, 1996).

The O_2 consumption is attributed to oxic degradation of organic matter (reaction 1, Table 1) and the reoxidation of the products from the anaerobic degradation of organic matter (Canfield et al., 1993). The observed thickness of the oxic layer depends directly on the C_{org} content in the surface sediment.

The peak of nitrate and nitrite in the oxic layer is attributed to the succession of reactions that lead to the bacterial nitrification of organic N (reaction 1, Table 1) or ammonia that diffuses from below (reaction 6, Table 1). The consumption of nitrate below the oxic layer is due to the bacterial denitrification (reaction 2, Table 1). Nitrite is an intermediate step in the formation in nitrate, and the presence of two peaks at the top and the bottom of the oxic layer of Stn. I suggests that nitrate is produced from reaction 1 at the top, and from reaction 6 just below. NO_3^- profile exhibit curvature throughout the oxic sediment layer of Stn. I, and hence imply that nitrate and oxygen respiration is taking place throughout much of the oxic layer. It is likely that the sediment investigated was not homogeneous, but instead had suboxic zones within its upper layer that allowed denitrification (Brandes and Devol, 1995).

NH_4^+ is produced from anaerobic mineralization of organic-N (reactions 4 and 5, Table 1). The production of dissolved Mn^{2+} and Fe^{2+} in anaerobic sediments is attributed to the dissimilatory reduction of

Table 1
List of reactions considered in this work

	Reaction number
Depth sequence of bacterially-mediated oxidation of organic matter (Froelich et al., 1979; De Lange, 1986) (O.M. = $C_{106}H_{263}O_{110}N_{16}P$)	
Oxygen consumption by oxic respiration and nitrate production $138O_2 + O.M. + 18HCO_3^- \rightarrow 124CO_2 + 16NO_3^- + HPO_4^{2-} + 140H_2O$	(1)
Nitrate consumption by denitrification $94.4NO_3^- + O.M. \rightarrow 13.6CO_2 + 92.4HCO_3^- + 55.2N_2 + 84.8H_2O + HPO_4^{2-}$	(2)
Reduction of Mn-oxides by anaerobic respiration $236MnO_2 + O.M. + 364CO_2 + 104H_2O \rightarrow 470HCO_3^- + 8N_2 + 236Mn^{2+} + HPO_4^{2-}$	(3)
Reduction of Fe-oxides and production of ammonia $424Fe(OH)_3 + O.M. + 740CO_2 \rightarrow 846HCO_3^- + 424Fe^{2+} + 16NH_3 + 320H_2O + HPO_4^{2-}$	(4)
Production of sulfide and ammonia by sulfatoreduction $53SO_4^{2-} + O.M. \rightarrow 39CO_2 + 67HCO_3^- + 16NH_4^+ + 53HS^- + 39H_2O + HPO_4^{2-}$	(5)
Production of nitrate by nitrification $NH_4^+ + 2O_2 \rightarrow NO_3^- + 2H^+ + H_2O$	(6)
Oxidation of Mn^{2+} with oxygen $2Mn^{2+} + O_2 + 2H_2O \rightarrow 2MnO_2 + 4H^+$ $4Mn^{2+} + O_2 + 6H_2O \rightarrow 4MnOOH + 8H^+$	(7)
Oxidation of Mn^{2+} with nitrate $5Mn^{2+} + 2NO_3^- + 4H_2O \rightarrow 5MnO_2 + N_2 + 8H^+$ $10Mn^{2+} + 2NO_3^- + 14H_2O \rightarrow 10MnOOH + N_2 + 18H^+$	(8)
Oxidation of Fe^{2+} with nitrate $5Fe^{2+} + NO_3^- + 12H_2O \rightarrow 5Fe(OH)_3 + 1/2N_2 + 9H^+$	(9)
Oxidation of Fe^{2+} with Mn-oxides $Fe^{2+} + MnOOH + H_2O \rightarrow Fe(OH)_3 + Mn^{2+}$ $2Fe^{2+} + MnO_2 + 4H_2O \rightarrow 2Fe(OH)_3 + Mn^{2+} + 2H^+$	(10)
Reduction of Mn-oxide with ammonia to give dinitrogen $3/2MnO_2 + NH_4^+ + 2H^+ \rightarrow 3/2Mn^{2+} + 1/2N_2 + 3H_2O$ $3MnOOH + NH_4^+ + 5H^+ \rightarrow 3Mn^{2+} + 1/2N_2 + 6H_2O$	(11)
Reduction of Mn-oxide with ammonia, production of nitrate $8MnOOH + NH_4^+ + 14H + \rightarrow 8Mn^{2+} + NO_3^- + 13H_2O$ $4MnO_2 + NH_4^+ + 6H^+ \rightarrow 4Mn^{2+} + NO_3^- + 5H_2O$	(12)

manganese and iron oxides by bacteria (reactions 3 and 4, Table 1). The peak of particulate Mn extracted by ascorbate or HCl can be attributed to detrital Mn-oxides and authigenic Mn-oxides precipitate from the oxidation of dissolved Mn^{2+} that diffuses from below (Sundby, 1977). The difference between Mn_{ASC} and Mn_{HCl} must be due to the higher efficiency of HCl to dissolve the Mn(III,IV) particles in comparison with the reductive dissolution with ascorbate. In St. I, A, and B, the concentration decreases abruptly below the oxic front, reaching values close to zero, which indicate that the Mn-oxides are totally reduced. In stations C and D, concentrations decrease more gradually, probably as the consequence of sediment mixing by bioturbation. Mn_{ASC} decreases to values close to zero, whereas Mn_{HCl} remains at concentrations above 5 μmol/g, which indicates that some Mn is buried in the solid fraction as an acid leachable phase. The carbonate fraction is dissolved by 1N HCl extraction, but not by ascorbate extraction (pH = 8). Therefore, the removal of dissolved Mn at depth in St. C, and D could be related to the precipitation of secondary Mn-containing carbonates. The precipitation of authigenic carbonates is favoured by the production of alkalinity linked to anaerobic mineralization of organic carbon (Mucci et al., 1999).

The distribution of of Fe_{ASC} is consistent with the assumption that the ascorbate reagent extracts only

the amorphous oxides (Kostka and Luther, 1994). The concentration is highest near the oxic layer and decreases below. Amorphous oxide phases may be used as terminal electron acceptors in bacterial oxidation of organic carbon or they may react with reduced sulfur to form FeS. The first hypothesis is supported by the occurrence of a peak of dissolved Fe(II) at the depth where Fe_{ASC} decreases. Iron from FeS can be extracted with the ascorbate solution. This may explain the presence of Fe_{ASC} in the anoxic part of the cores, especially in St. E, D, and C, where total solid S is abundant. Fe_{HCl} profiles are approximately parallel to the Fe_{ASC} profiles, which suggests that the decrease in Fe_{HCl} profiles observed below the oxic layer corresponds to the reduction of the most reactive fraction of solid Fe(III) (the Fe_{ASC} fraction). The additional part can consist of a less reactive fraction toward sulfide (Canfield et al., 1992) or toward bacterial reduction (Postma and Jakobsen, 1996).

The presence of particulate sulfur in continental margin sediments can be mostly attributed to authigenic iron-sulfide minerals that precipitate during the degradation of organic matter by sulfate-reduction (reaction 5, Table 1) (Berner, 1971; Jørgensen, 1982). The first compound that generally forms is amorphous FeS. It is subsequently converted to more crystalline pyrite (Berner, 1970; Schoonen and Barnes, 1991). The diluted presence of FeS in the deep sediments of St. I, A, and B was confirmed by the presence of small black dots at the surface of the deeper sediment slices. In stations E, C, and D, the presence of FeS was confirmed, first because these sediments were black or dark grey below 5 cm depth, and second, because of the characteristic odour of H_2S that emanated from the vial during the 1N HCl leaching. FeS is not stable in the presence of oxygen. Therefore, the particulate sulfur which was measured in the oxic part of St. E, C, and D can arise from the advective upward transport by bioturbation of refractory pyrite produced deeper in the sediment.

4.3. Specific features of stations B and E

The solid fraction of Stn. E has the same distribution as stations C and D in the bottom of the core. At the top, however, the sediment reveals specific features, which can be explained by the recent deposition of a sediment layer by a gravity flow, as suggested from the ^{210}Pb data. The top 2 cm are enriched in S_{tot}, and depleted in C_{org}. This is typical of aged sediments. The 3–5 cm layer presents a peak of extractable Mn and Fe, which can be interpreted as the earlier sediment–water interface. These subsurface peaks of oxidized particles should disappear in a few years (e.g. Mucci and Edenborn, 1992). It suggests that the top layer has been deposited recently.

Stn. B core contains a layer between 12 and 14 cm, far below the oxygen penetration depth we measured, which is depleted in reduced compounds and enriched in nitrate and nitrite. This suggests that this layer contained trace amount of oxygen, which could be related to bioirrigation.

4.4. Other reactions

There is no doubt that the sequence of reactions related to the oxidation of organic matter, and the re-oxidation of reduced species produced in the anaerobic zone that diffuse in the oxic layer are the major processes that explain the measured profiles. Recent works suggest, however, that the web of reactions that leads to the reduction of oxidizing compounds or the oxidation of dissolved reduced species is more complex. For example, manganese dioxide may be reduced directly by ammonia (Luther et al., 1997; Aller et al., 1998; Hulth et al., 1999). Nitrate may also be reduced to dinitrogen by Mn^{2+} and Fe^{2+} (Sørensen et al., 1987; Postma, 1990; Aller, 1994; Schulz et al., 1994; Murray et al., 1995; Luther et al., 1997,1998). Manganese oxides and oxyhydroxides are also oxidants for Fe^{2+} (Myers and Nealson, 1988; Postma, 1985) and S(-II) (Burdige and Nealson, 1987; Aller and Rude, 1988; Yao and Millero, 1996; Canfield et al., 1993), and iron oxides and oxyhydroxides are oxidants for sulfide (Rickard, 1974; Pyzik and Sommer, 1981). The profiles we have obtained for the sediments of the Bay of Biscay allow us to check the occurrence of these secondary redox reactions, particularly those in which Mn, Fe, and N compounds are involved. The potential importance of these reactions will be evaluated using a model of vertical fluxes of the reactive species.

4.4.1. Oxidation of Mn^{2+}

Dissolved Mn^{2+} is present in the anoxic part of

the cores. The concentrations drop below the detection limit at the bottom of the oxygen-bearing layer. It suggests that O_2 is the primary oxidant of Mn^{2+}, which diffuses upwards, according to reaction (7) (Table 1). This oxidation pathway is thermodynamically favourable (Stumm and Morgan, 1996). The kinetics is extremely slow in synthetic waters (Diem and Stumm, 1984) but becomes orders of magnitude faster in natural waters containing Mn-bacteria or surface catalysts (Van der Weijden, 1975; Sung and Morgan, 1981). Recent studies based on high resolution microelectrode measurements (Luther et al., 1997) showed that in the Gulf of St. Lawrence sediments the Mn^{2+} profile did not overlap the profile of O_2. The layer depleted in O_2 and Mn^{2+} was up to 14 mm thick. Luther et al. (1997) suggested that nitrate was the primary oxidant for Mn^{2+}. This is possible when the product is dinitrogen, according to reaction 8 (Table 1). Our profiles have a good vertical resolution for O_2, but only a 5 mm resolution at the top of cores for Mn^{2+}. At this resolution, both profiles overlap. One must notice that the horizon in which O_2 or Mn^{2+} exist can exhibit topography within the three dimensions sediment matrix (Luther et al., 1998). Therefore a given strata corresponding to a sediment slice of 0.5 or 1 cm can mix pore water compounds that actually do not co-exist. Just below the O_2 front, we also observe that Mn^{2+} is present together with nitrate. In Stn. I, the overlapping occurs within five slices which suggests that both species actually co-exist, and can cumulate in pore waters without reacting mutually. Therefore, O_2 is a better candidate in these sediments for the primary oxidation of diffusing Mn^{2+}.

Dissolved Mn^{2+} is produced by the reductive dissolution of Mn-oxides in the anaerobic part of the sediment. That is why the maximum concentrations are observed at the depth where extracted Mn-oxides contents decrease sharply at stations B, C, D, and E. At St. I and A, however, the maximum concentrations are observed at the bottom of the cores. Despite the drastic decline of particulate Mn at the oxic front, specifically in Stn. I, we observe no peak of dissolved Mn^{2+}. This suggests that most of Mn-oxides are reduced very close to the depth where oxygen disappears, or even at a level where oxygen is still present, and that produced Mn^{2+} is immediately re-oxidized with O_2.

4.4.2. Oxidation of Fe^{2+}

Dissolved Fe^{2+} is detected generally deeper than 1 cm below the oxic front. It is possible that some undetected trace amount of dissolved O_2 could act as primary oxidant for Fe^{2+}. However, Fe^{2+} appears generally at the depth where nitrate becomes undetectable. This indicates that nitrate could be the primary oxydant for Fe^{2+} according to the reaction 9 (Table 1). In cores D and B, however, nitrate appears in the sediment strata located between 5 and 6 cm depth. This interval also contains dissolved Fe^{2+}. Mn-oxide can also efficiently oxidize Fe^{2+} in marine sediments (Myers and Nealson, 1988; Postma, 1985), or in Mn- and Fe-rich anoxic basins (e.g. Anschutz and Blanc, 1995) (reaction 10, Table 1). In the bioturbated cores C and D, dissolved Fe^{2+} is still present in the intervals which contain Mn_{ASC} concentrations far above the background level measured at the bottom of the cores. The co-existence of dissolved Fe(II) with Mn_{ASC} or nitrate in the analysed samples does perhaps not exist in the sediment, because the sampling procedure averages the three dimensions topography of redox fronts or possible microniches. Therefore, both nitrate or Mn-oxides can be the effective barrier for upward diffusing Fe^{2+}.

4.4.3. Oxidation of ammonia

Ammonia profiles show smooth gradients from the bottom to the oxic layer. The classical explanation for this is that ammonia is produced from the anaerobic mineralization of organic N at depth. In the oxic layer, nitrifying bacteria oxidize ammonia with oxygen to nitrite and nitrate, and nitrate is subsequently reduced anaerobically to dinitrogen by denitrifying bacteria. However, recent publications show that ammonia may also be oxidized directly by manganese oxide, either to dinitrogen in the presence of oxygen (Luther et al., 1997), or to nitrate in anaerobic sediments (Aller et al., 1998; Hulth et al., 1999; Anschutz et al., 2000) (reactions 11 and 12, Table 1). Reaction 12 may explain the presence of nitrate in the anaerobic part of bioturbated sediments (e.g. Stn. D), where Mn-oxides are advected in layers enriched in ammonia. At the bottom of the oxic layer where ammonia is oxidized, Mn-oxides represent a quantity of oxidizing agent, which is many orders of magnitude higher than the amount of dissolved oxygen.

Table 2
Vertical fluxes of reactive species in μmol/cm^2/year (negative and positive values correspond to downward and upward fluxes, respectively)

Station	O_2[a]	NO_3^-	NH_4^+	Mn^{2+}	Fe^{2+}	Fe_{ASC}[b]	Mn_{HCl}[b]
I	−109	2.2; −1.5	1.3	0.2; /	0.6	−2	−1.5
A	−44	2.2; −1.3	1.1	0.2; /	0.3	−1.7	−0.5
B	−166	4.6; −1.9	1.9	2.6; −0.3	2.2		−1
E	−144	2.1; −3.4	3.5	4.5: −1,7	1.5		
C	−98	2.2; −2.0	4.3	5.6; −1.1	3.9		
D	−217	4.0; −2.9	11.5	6.2; −1,1	1.5		

[a] Flux of O_2 across the sediment–water interface.
[b] The downward flux of reactive particles has been calculated from the accumulation rate deduced from ^{210}Pb data and the averaged concentration of Fe_{ASC} and Mn_{HCl} in the enriched top layer.

For example, at about 4 cm depth in Stn. I, there is approximately 50 μmol of Mn-oxide per cm^3, whereas oxygen represents only a few nanomoles. Therefore, chemical reduction of Mn-oxide through reactions 11 or 12 may dominate and compete with both nitrification (reaction 6) and the dissimilatory reduction of Mn-oxides (reaction 3).

4.4.4. Flux calculations

The Mn-oxide reduction by ammonia can only be quantitatively important if the upward flux of ammonia is higher than the downward flux of Mn-oxide, taking the reaction stoichiometry into account. The same reasoning can be applied for the oxidation of Mn^{2+} with oxygen. We can estimate the downward particle flux of undisturbed sediments from the ^{210}Pb data. The fluxes of species dissolved in pore waters can be calculated, assuming transport by molecular diffusion, from the concentration gradients according to Fick's first law:

$$J = -\phi D_s \mathrm{d}C/\mathrm{d}X \quad (1)$$

where J is the flux, ϕ is the porosity, dC/dX is the concentration gradient, and D_s is the bulk sediment diffusion coefficient corrected for tortuosity, i.e. $D_s = D_0/\theta^2$ where θ is the tortuosity and D_0 is the diffusion coefficient in water (Berner, 1980). D_0 values were obtained from Li and Gregory (1974) and the value of θ^2 is assumed to equal to $1 - \ln(\phi^2)$ (Boudreau, 1996). An estimation of the diffusive flux of O_2 across the sediment–water interface and within the sediment was calculated from a curve-fitting approach as described by Rasmussen and Jørgensen (1992). Briefly, parabola were visually fitted with parts of the oxygen profile. The coefficients of each parabola were calculated (i.e. $C(z) = az^2 + bz + c$). The flux J was calculated from the linear coefficient (b) according to:

$$J = -b\phi D_s \quad (2)$$

The details of this method are explained by Rasmussen and Jørgensen (1992), or De Wit et al. (1995) DeWit et al. (1995). A straight line was preferred if linear regression gave better description than quadratic regression in some parts of the oxygen profiles, and a constant downward flux of oxygen was calculated according to Ficks first law [Eq. (1)]. The results of all the flux calculations are presented in Table 2 and visualized in Fig. 5 for Stn. I. We find

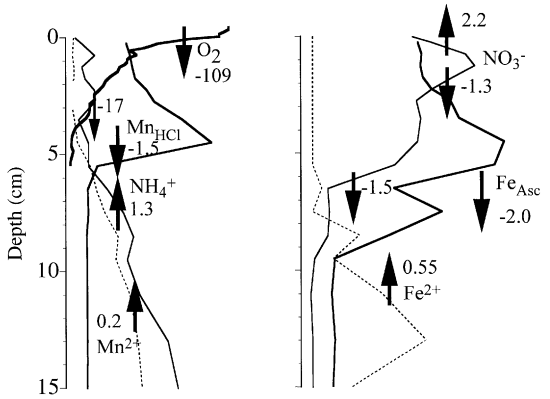

Fig. 5. Vertical fluxes of reactive species in modern sediments of station I. Fluxes were calculated with a molecular diffusion model for species dissolved in pore waters, and deduced from the calculated accumulation rate for particulate Mn_{HCl} and Fe_{ASC}.

that the downward flux of particulate Mn is 1.5 μmol/cm^2/yr at Stn. I. The opposite flux of ammonia is 1.3 μmol/cm^2/yr. The stoichiometry of reactions 11 or 12 (Table 1) shows that one NH_4^+ can reduce from 1.5 to 8 Mn-oxides, depending of the reaction. This means that all the Mn(III,IV) oxides may theoretically be reduced by ammonia in St. I. This pathways can compete with, or even short-circuit the dissimilatory reduction of Mn-oxides (reaction 3, Table 1), allowing more organic matter to be mineralized through anaerobic processes (reactions 4 and 5, Table 1). In fact, a great part of the ammonia flux remains available for nitrification (reaction 6, Table 1) after the complete reduction of Mn-oxides. The downward flux of Mn-oxides at the redox front must correspond to the rate of Mn^{2+} production, i.e. 1.5 μmol/cm^2/yr. The downward flux of O_2 at the bottom of the oxic layer is 17 μmol/cm^2/yr, which is large enough to oxidize the produced Mn^{2+} (reaction 7) and also the remaining ammonia (reaction 6). This can explain the absence of a peak at the redox front in the profile of dissolved Mn^{2+}. Therefore, a sustained suite of reactions can occur at the bottom of the oxic layer, where Mn-oxides are reduced by ammonia in Mn^{2+}, which is directly re-oxidized with oxygen. This corresponds, in fact, to a catalytic oxidation of ammonia by oxygen, with Mn-oxides as intermediate reagent, as described by Luther et al. (1997). We arrive at the same conclusions from the flux calculations for stations A and B. The particles of the other stations are mixed by bioturbation or disrupted by sedimentological events. Therefore, it is not possible to obtain the downward flux of Mn-oxides in order to compare it with the ammonia flux.

The upward flux of the Mn^{2+} that diffuses from the bottom of the core is 0.2 μmol/cm^2/yr in Stn. I (Fig. 5). The quantity of particulate Mn extracted with HCl, which is incorporated in a 1 cm^2 section of the oxic layer is about 120 μmol. Therefore, 600 years are needed to form the peak of Mn_{HCl} from the diffusing Mn^{2+}. However, the 4.5 cm thick oxic layer corresponds approximately to 100 years of deposition, according to the mass accumulation rate estimated with the ^{210}Pb data. Thus, the peak of particulate Mn results from the accumulation of detrital Mn over a long period of time and its continuous reworking at the redox front.

The flux of O_2 across the sediment–water interface (Table 2) corresponds to the calculated diffusive flux. It has been observed that the oxygen flux calculated from the pore water profile is lower than that measured during sediment incubation with benthic chambers (Rowe and McNichol, 1991). Discrepancy between calculated and measured values suggests that oxic respiration by macrobenthos present in the supernatant water column, which is not reflected in a one-dimension oxygen profile, occurred in incubated cores. Gundersen and Jørgensen (1990) also found that in marine sediments with shallow oxygen penetration, diffusive fluxes can be underestimated by a factor of up to 2.5 when the roughness, i.e. the surface area of the sediment–water interface was not taken into account. We presume, however, that the calculation based on pore water profiles gives values that predominantly comprise the fraction due to microorganisms and oxidation reactions that are dependent on the diffusive oxygen flow. This opinion is supported by recent observations that have shown that total oxygen uptake in the deep sea measured by benthic chambers equals or exceeds the calculated diffusive flux, with the actual difference being positively correlated with macrofaunal densities (Archer and Devol, 1992; Glud et al., 1994).

The fluxes of O_2 we measured are not directly dependent of the depth of the station or the oxygen penetration depth into the sediment. For example, in Stn. I located at 2800 m depth, the flux is 109 μmol/cm^2/year, which is of the same order of magnitude as that in Stn. C, located at 280 m depth. Oxygen uptake within the sediment is governed by the benthic microbial respiration (reaction 1, Table 1) and by oxidation of reduced species diffusing from the anoxic part of the sediment. In the sulfide-rich sediments of stations C, D, and E, a non-quantified, proportion of O_2 must be used for the oxidation iron sulfides, which can be transported into the oxic zone by bioturbation. This proportion can be important in coastal sediments (Canfield et al., 1993), that is why we have not quantified oxic respiration in these cores. We have also shown that ammonia is oxidized by oxygen, but a part of the oxidation reaction occurs with the reduction of Mn(III, IV) oxides and the re-oxidation of Mn^{2+} with oxygen as intermediate processes. In the studied cores Mn^{2+} appears to be directly oxidized by oxygen. Our data suggest that Fe^{2+} can be oxidized by nitrate. Therefore, the flux of Fe^{2+} does

Table 3
Rates of oxygen consumption deduced from pore water gradients and calculated rates of nitrate production (in μmol/cm^2/yr)

	Station I	Station A	Station B
O_2[a]	2.7	2.3	5.1
O_2[b]	106.3	41.7	160.9
NO_3^- production[c]	13.6	5.9	20.6
Σ Flux NO_3^-[d]	3.7	3.5	6.5

[a] Rate of oxygen consumption for the oxidation of upward diffusing ammonia and dissolved manganese.
[b] Rate of oxygen consumption through the mineralization of organic matter.
[c] Production of nitrate through oxidation of diffusing ammonia and oxidation with oxygen of organic N, assuming that the mineralized organic matter has a C/N ratio of 6.6.
[d] Sum of diffusive fluxes of nitrate away from the oxic layer.

perhaps not enter directly into the budget of oxygen consumption. The part of oxygen used for oxic respiration in stations I, A, and B corresponds, therefore, to the diffusive flux of oxygen minus the upward fluxes of ammonia and dissolved Mn, corrected for the stoichiometry of the reactions. The nitrification of one NH_4^+ corresponds to the uptake of two O_2, and the total oxidation of one Mn^{2+} in Mn(IV) oxide corresponds to the consumption of 0.5 O_2. Table 3 shows the calculated rates of O_2 respiration and O_2 used for other processes. The oxic respiration corresponds to more than 93% of the total O_2 flux in stations I, A, and B. The oxidation of organic matter with O_2 produces NO_3^- according to reaction 1 (Table 1). This explains the positive peaks at the top of the oxic layer of the sediment cores. The production of NO_3^- by this pathway can be estimated assuming that the organic matter that is mineralized at the sediment–water interface has a C/N ratio of 6.6, which corresponds to the average composition of marine planktonic organisms (Redfield et al., 1963). This hypothesis is realistic, because fresh marine detritus corresponds to the most labile fraction of organic matter. The respiration of one O_2 corresponds to the production of 16/138 NO_3^-. Additional nitrate is also produced from the oxidation of ammonia that diffuses toward the oxic front at a rate that corresponds roughly to the calculated upward flux of ammonia. The rates of nitrification presented in Table 3 are much larger for the oxic mineralization of organic N than for nitrification of ammonia.

The total produced nitrate either diffuses out of the sediment to the water column, or may be reduced at depth by Fe^{2+} (reaction 9) or through denitrification (reaction 2). Therefore, the nitrate production in the oxic layer should be balanced by the nitrate fluxes out of this layer. The upward nitrate flux was calculated assuming a linear concentration gradient between the middle of the first sampling interval (0–5 mm) and the sediment surface. The calculated rate of nitrate production largely exceeds the sum of fluxes of nitrate away from the oxic layer by a factor of 2–4 (Table 3). This can be due to an overestimation of N content of organic matter that is mineralized. However, the C/N ratio of settling organic matter rarely exceeds the Redfield ratio by a factor larger than 2 (Ruttenberg and Goñi, 1997). Our calculations suggest, therefore, that the denitrification process occurs in anoxic microenvironments located in the oxic layer (Brandes and Devol, 1995), or it is carried out by aerobic bacteria (e.g. Frette et al., 1997; Lloyd et al., 1987; Robertson et al., 1989). The latter would eliminate the need to transport all nitrate from the aerobic to the anaerobic zone of the sediment.

5. Conclusions

We have defined the diagenetic processes that occur in modern sediments of the Bay of Biscay from vertical profiles of redox species and excess ^{210}Pb data. The shallowest stations D and C contain more than 2% C_{org}. These stations are deeply bioturbated. The deeper stations I, A, and B contain less C_{org} and are much less bioturbated. St. E located in the Capbreton canyon has known a recent sedimentological event corresponding to a turbidity current deposition of a 3 cm thick sediment layer previously transformed by early diagenetic processes. Despite these environmental differences it was possible to recognize the classical vertical sequence of redox reaction linked to the bacterially-mediated oxidation of organic matter in all the stations.

We have calculated the vertical fluxes of redox species from the composition gradients in pore waters and the ^{210}Pb data. From the flux data and the shape of the profiles we point out that several secondary redox

reactions could influence indirectly the pathway of organic matter mineralization.

We have calculated that all of the Mn-oxides can be reduced by ammonia in stations I, A, and B. If that chemical reaction occurs, it can directly compete with, or even short-circuit, the dissimilatory reduction of Mn-oxides. The reduction of Mn-oxides to Mn^{2+} by ammonia can occur in the presence of small amounts of oxygen, at the bottom of the oxic layer. This process can prevent the build-up of a peak of dissolved Mn^{2+}, since Mn^{2+} is directly reoxidized by oxygen. Therefore, the detrital Mn that cumulates during sedimentation is continuously recycled at the oxic front. In undisturbed sediments like at Stn. I, this promotes the formation of a surface layer, which becomes very enriched in particulate Mn. In disturbed sediments, some Mn-oxide particles are carried down in the anoxic part. Their reduction produces a peak of dissolved Mn^{2+} below the oxic front. At depth, Mn^{2+} can be partly trapped as an authigenic carbonate phase. Our data and flux calculations suggest that the primary oxidant for dissolved Fe^{2+} is nitrate. If this process takes place, it leaves less nitrate for anaerobic bacterial denitrification. The theoretical production of nitrate in the oxic layer has been estimated in undisturbed sediments from the flux of oxygen at the sediment–water interface. The calculated value is far above the flux of nitrate away from the oxic layer, which suggests that nitrate consumption occurs in anaerobic microniches or in the presence of oxygen.

We showed that the chemical profiles in modern sediments of the Bay of Biscay can be explained by the classical sequence of redox reactions that occur during early diagenesis. However, we must keep in mind that some alternative reactions, which are thermodynamically favourable, can also explain some profiles.

Acknowledgements

This research is the contribution 1380 of the CNRS UMR 5805 'Environnements et Paléoenvironnements Océaniques', and was funded by the program PROOF of the Institut National des Sciences de l'Univers and the Région Aquitaine. Karine Dedieu contributed to the laboratory analyses. We thank the crew of the 'Côtes de la Manche' and all the participants of the Oxybent missions.

References

Aller, R.C., 1994. The sedimentary Mn cycle in Long Island Sound: Its role as intermediate oxidant and the influence of bioturbation, O2, and Corg flux on diagenetic reaction balances. J. Mar. Res. 52, 259–295.

Aller, R.C., Rude, P.D., 1988. Complete oxidation of solid phase sulfides by manganese and bacteria in anoxic marine sediments. Geochim. Cosmochim. Acta 52, 751–765.

Aller, R.C., Hall, P.O.J., Rude, P.D., Aller, J.Y., 1998. Biogeochemical heterogeneity and suboxic diagenesis in hemipelagic sediments of the Panama Basin. Deep-Sea Res. I 45, 133–165.

Anderson, L., 1979. Simultaneous spectrophotometric determination of nitrite and nitrate by flow injection analysis. Anal. Chim. Acta 110, 123–128.

Anschutz, P., Blanc, G., 1995. Chemical mass balances in metalliferous deposits from the Atlantis II Deep (Red Sea). Geochim. Cosmochim. Acta 59, 4205–4218.

Anschutz, P., Zhong, S., Sundby, B., Mucci, A., Gobeil, C., 1998. Burial efficiency of phosphorus and the geochemistry of iron in continental margin sediments. Limnol. Oceanogr. 43, 53–64.

Anschutz, P., Hyacinthe, C., Carbonel, P., Jouanneau, J.M., Jorissen, F.J., 1999. La distribution du phosphore inorganique dans les sédiments modernes du Golfe de Gascogne. C. R. Acad. Sci. Paris 328, 765–771.

Anschutz, P., Sundby, B., LeFrançois, L., Luther, I.I.I.G.W., Mucci, A., 2000. Interaction between metal oxides and the species of nitrogen and iodine in bioturbated marine sediments. Geochim. Cosmochim. Acta 64, 2751–2763.

Archer, D., Devol, A., 1992. Benthic oxygen fluxes on the Washington shelf and slope: a comparison of in situ microelectrode and chamber fluxes. Limnol. Oceanogr. 37, 614–629.

Berner, R.A., 1970. Sedimentary pyrite formation. Am. J. Sci. 268, 1–23.

Berner, R.A., 1971. Principles of Chemical Sedimentology. McGraw-Hill, New York.

Berner, R.A., 1980. Early Diagenesis: A Theoretical Approach. Princeton University Press, Princeton, NJ.

Boudreau, B.P., 1996. The diffusive tortuosity of fine-grained unlithified sediments. Geochim. Cosmochim. Acta 60, 3139–3142.

Brandes, J.A., Devol, A.H., 1995. Simultaneous nitrate and oxygen respiration in coastal sediments: Evidence for discrete diagenesis. J. Mar. Res. 53, 771–797.

Burdige, D.J., Gieskes, J.M., 1983. A pore water/solid phase diagenetic model for manganese in marine sediments. Am. J. Sci. 283, 29–47.

Burdige, D.J., Nealson, K.H., 1987. Microbial manganese reduction by enrichment cultures from coastal marine sediments. Appl. Environ. Microbiol. 50, 491–497.

Canfield, D.E., Raiswell, R., Bottrell, S., 1992. The reactivity of sedimentary iron minerals toward sulfide. Am. J. Sci. 292, 659–683.

Canfield, D.E., Jørgensen, B.B., Fossing, H., Glud, R., Gundersen, J., Ramsing, N.B., Thamdrup, B., Hansen, J.W., Nielsen, L.P., Hall, P.O.J., 1993. Pathways of organic carbon oxidation in three continental margin sediments. Mar. Geol. 113, 27–40.

De Lange, G.J., 1986. Early diagenetic reaction in interbeded pelagic and turbiditic sediments in the Nares Abyssal Plain (Western North Atlantic): consequences for the composition of sediment and interstitial water. Geochim. Cosmochim. Acta 50, 2543–2561.

De Wit, R., Relexans, J.-C., Bouvier, T., 1995. Microbial respiration and diffusive oxygen uptake of deep-sea sediments in the Southern Ocean (ANTARES-I cruise). Deep-Sea Res. II 44, 1053–1068.

Diem, D., Stumm, W., 1984. Is dissolved Mn^{2+} being oxidized by O2 in absence of Mn-bacteria of surface catalysts? Geochim. Cosmochim. Acta 48, 1571–1573.

Ferdelman, T.G., 1988. The distribution of sulfur, iron, manganese, copper and uranium in salt marsh sediment cores as determined by sequential extraction methods. MSc Thesis, University of Delaware, USA.

Frette, L., Gejlsbjerg, B., Westermann, P., 1997. Aerobic denitrifiers isolated from an alternating activated sludge system. FEMS Microbiol. Ecol. 24, 363–370.

Froelich, P.N., Klinkhammer, G.P., Bender, M.L., Luedke, N.A., Heath, G.R., Cullen, D., Dauphin, P., Hammond, D., Hartman, B., Maynard, V., 1979. Early oxidation of organic matter in pelagic sediments of the Eastern Equatorial Atlantic: suboxic diagenesis. Geochim. Cosmochim. Acta 43, 1075–1090.

Glud, R.N., Gundersen, J.K., Jørgensen, B.B., Revsbech, N.P., Schulz, H.D., 1994. Diffusive total oxygen uptake of deep-sea sediments in the eastern South Atlantic Ocean: in situ and laboratory measurements. Deep-Sea Res. I 41, 1767–1788.

Gundersen, J.K., Jørgensen, B.B., 1990. Microstructure of diffusive boundary layers and the oxygen uptake of the sea floor. Nature 345, 604–607.

Hall, P.O.J., Aller, R.C., 1992. Rapid, small-volume flow injection analysis for (CO2 and NH^{4+} in marine and freshwaters. Limnol. Oceanogr. 37, 1113–1119.

Helder, W., Bakker, J.F., 1985. Shipboard comparison of micro- and mini electrodes for measuring oxygen distribution in marine sediments . Limnol. Oceanogr. 30, 1106–1109.

Hulth, S., Aller, R.C., Gibert, F., 1999. Coupled anoxic nitrifcation/manganese reduction in marine sediments. Geochim. Cosmochim. Acta 63, 49–66.

Hulthe, G., Hulth, S., Hall, P.O.J., 1998. Effect of oxygen on degradation rate and labile organic matter in continental margin sediments. Geochim. Cosmochim. Acta 62, 1319–1328.

Jørgensen, B.B., 1982. Mineralization of organic matter in the sea-bed. The role of sulfate reduction. Nature 296, 643–645.

Kostka, J.E., Luther, I.I.I.G.W., 1994. Partitioning and speciation of solid phase iron in saltmarsh sediments. Geochim. Cosmochim. Acta 58, 1701–1710.

Latouche, C., Jouanneau, J.M., Lapaquellerie, Y., Maillet, N., Weber, O., 1991. Répartition des minéraux argileux sur le plateau continental Sud-Gascogne. Oceanologica Acta 11, 155–161.

Li, Y.H., Gregory, S., 1974. Diffusion of ions in seawater and in deep-sea sediments. Geochim. Cosmochim. Acta 38, 703–714.

Lloyd, D., Boddy, L., Davies, K.P.J., 1987. Persistence of bacterial denitrification capacity under aerobic conditions: the rule rather than the exception. FEMS Microbiol. Ecol. 45, 185–190.

Luther, I.I.I.G.W., Sundby, B., Lewis, G.L., Brendel, P.J., Silverberg, N., 1997. Interactions of manganese with the nitrogen cycle: alternative pathways for dinitrogen formation. Geochim. Cosmochim. Acta 61, 4043–4052.

Luther, I.I.I.G.W., Brendel, P.J., Lewis, B.L., Sundby, B., Lefrançois, L., Silverberg, N., Nuzzio, D., 1998. Oxygen, manganese, iron, iodide, and sulfide distributions in pore waters of marine sediments measured simultaneously with a solid state voltammetric microelectrode. Limnol. Oceanogr. 43, 325–333.

Mucci, A., Edenborn, H.M., 1992. Influence of an organic-poor landslide deposit on the early diagenesis of iron and manganese in a coastal marine sediment. Geochim. Cosmochim. Acta 56, 3909–3921.

Mucci, A., Sundby, B., Gehlen, M., Arakaki, T., Silverberg, N., 1999. The fate of carbon in continental shelf sediments: a case study. Deep Sea Res. II 47, 733–760.

Murray, J.W., Codispoti, L.A., Friederich, G.E., 1995. Oxidation-reduction environments: The suboxic zone of the Black Sea. In: Huang, C.P., O'Melia, C.R., Morgan, J.J., (Eds.), Aquatic chemistry: Interfacial and Interspecies Processes. American Chemical Society, 244, 157–176.

Myers, C.R., Nealson, K.H., 1988. Microbial reduction of manganese oxides: interactions with iron and sulfur. Geochim. Cosmochim. Acta 52, 2727–2732.

Postma, D., 1985. Concentration of Mn and separation from Fe in sediments—I. Kinetics and stoichiometry of the reaction between birnessite and dissolved Fe(II) at 10°C. Geochim. Cosmochim. Acta 49, 1023–1033.

Postma, D., 1990. Kinetics of nitrate reduction by detrital Fe(II)-silicates. Geochim. Cosmochim. Acta 54, 903–908.

Postma, D., Jakobsen, R., 1996. Redox zonation: Equilibrium constrains on the Fe(III)/SO_4-reduction interface. Geochim. Cosmochim. Acta 60, 3169–3175.

Pyzik, A.J., Sommer, S.E., 1981. Sedimentary iron monosulfides: kinetics and mechanisms of formation. Geochim. Cosmochim. Acta 45, 687–698.

Rabouille, C., Gaillard, J.F., Relexans, J.C., Tréguer, P., Vincendeau, M.A., 1998. Recycling of organic matter in Antarctic sediments: A transect through the Polar front in the Southern Ocean (Indian Sector). Limnol. Oceanogr. 43, 420–432.

Rasmussen, H., Jørgensen, B.B., 1992. Microelectrode studies of seasonal oxygen uptake in a coastal sediment: role of molecular diffusion. Mar. Ecol. Prog. Ser. 81, 289–303.

Redfield, A.C., Ketchum, B.H., Richards, F.A., 1963. The influence of organisms on the composition of sea-water. In: Hill, M.N. (Ed.), The Sea. Interscience Publishers II, pp. 26–77.

Revsbech, N.P., 1983. In-situ measurements of oxygen profiles of sediments by use of oxygen microelectrodes. In: Gnaiger, F. (Ed.), Polarographic Oxygen Sensors. Springer, Berlin, pp. 265–273.

Revsbech, N.P., Jørgensen, B.B., 1986. Microelectrodes: their use

in microbial ecology. In: Advances in Microbial Ecology 9, Plenum Press, New York, pp. 293–352.

Rickard, D., 1974. Kinetics and mechanism of the sulfidation of goethite. Am. J. Sci. 274, 941–952.

Robertson, L.A., Cornelisse, R., de Vos, P., Hadioetomo, R., Kuenen, J.G., 1989. Aerobic denitrification in various heterotrophic nitrifiers. Antonie van Leeuwenhoek 56, 289–299.

Rowe, G.T., McNichol, A.P., 1991. Carbon cycling in coastal sediments: Estimating remineralisation in Buzzards Bay, Massachusetts. Geochim. Cosmochim. Acta 55, 2989–2991.

Ruttenberg, K.C., Goñi, M.A., 1997. Phosphorus distribution, C:N:P ratios, and d13Coc in arctic, temperate, and tropical coastal sediments: tools for characterizing bulk sedimentary organic matter. Mar. Geol. 139, 123–145.

Schoonen, M.A.A., Barnes, H.L., 1991. Mechanisms of pyrite and marcasite formation from solution: III – Hydrothermal processes. Geochim. Cosmochim. Acta 55, 3491–3504.

Schulz, H.D., Dahmke, A., Schnizel, U., Wallmann, K., Zabel, M., 1994. Early diagenetic processes, fluxes, and reaction rates in sediments of the South Atlantic. Geochim. Cosmochim. Acta 58, 2041–2060.

Sørensen, J., Jørgensen, B.B., Colley, S., Hydes, D.J., Thomson, J., Wilson, T.R.S., 1987. Depth localization of denitrification in a deep-sea sediment from the Madeira Abyssal Plain. Limnol. Oceanogr. 32, 758–762.

Stookey, L.L., 1970. Ferrozine—A new spectrophotometric reagent for iron. Anal. Chem. 42, 779–781.

Strickland, J.D.H., Parsons, T.R., 1972. A practical handbook of seawater analysis. Bull. Fish. Resour. Board Can. 167, 1–311.

Stumm, W., Morgan, J.J., 1996. Aquatic Chemistry. 3rd ed., Wiley and Sons, New York.

Sundby, B., 1977. Manganese-rich particulate matter in a coastal marine environment. Nature 270, 417–419.

Sung, W., Morgan, J.J., 1981. Oxidative removal of Mn(II) from solution catalysed by the g-FeOOH (lepidocrosite) surface. Geochim. Cosmochim. Acta 45, 2377–2383.

Van der Weijden, C.H., 1975. Sorption experiments relevative to the geochemistry of manganese nodules. PhD Thesis, University of Utrecht.

Wang, Y., Van Cappellen, P., 1996. A multicomponent reactive transport model of early diagenesis: application to redox cycling in coastal marine sediments. Geochim. Cosmochim. Acta 60, 2993–3014.

Yao, W., Millero, F.J., 1996. Oxidation of hydrogen sulfide by hydrous Fe(III) oxides in seawater. Mar. Chem. 52, 1–16.